Journal of Applied Polymer Science

Preparation and characterization of poly(*o*-anisidine) with the influence of surfactants on stainless steel by electrochemical polymerization as a counter electrode for dye-sensitized solar cells

Chandrasekaran Menaka, Paramasivam Manisankar, Thambusamy Stalin
Department of Industrial Chemistry, Photoelectrochemistry Laboratory, Alagappa University, Karaikudi 630003 Tamilnadu, India
Correspondence to: T. Stalin (E-mail: drstalin76@gmail.com)

ABSTRACT: Efficient fast electron transfer from counter electrode to an electrolyte is a key process during the operation of dye-sensitized solar cells (DSSCs). We introduce a surfactants assisted electro-polymerized poly(*o*-anisidine) (POA) counter electrodes (CE) for DSSCs. Commencing the electrochemical impedance spectroscopy, the POA/sodium dodecyl sulphate (SDS) CE exhibited very low series and charge-transfer resistance. This is due to high electrocatalytic activity confirmed by cyclic voltammetry, surface area and the conductivity of the stainless steel film. The photovoltaic performance of POA/SDS counter electrode shows an energy conversion efficiency of 2.5% under 1 sun illumination. Short-term stability test for POA/SDS point out that CE have almost uphold its initial performance. © 2015 Wiley Periodicals, Inc. J. Appl. Polym. Sci. **2015**, *132*, 42310.

KEYWORDS: conducting polymers; electrochemistry; surfactants

Received 3 February 2015; accepted 6 April 2015
DOI: 10.1002/app.42310

INTRODUCTION

A dye-sensitized solar cell (DSSC) was one of the promising candidates for inexpensive, eco-friendly and easy fabricates Photovoltaic technology.[1] Generally counter electrode (CE) is a conducting glass substrate coated with Pt, a catalytic material to speed up the reduction reaction of triiodide (I_3^-) to iodide ions. It is true that Pt is still the most efficient catalyst material for DSSCs.[2] However, platinum is a noble metal and relatively expensive. Consequently, the cost of the platinum CE was more than 40% of the whole DSSC cell cost apart from of its preparation method. In addition, to that a slow dissolution of platinum in I_3^-/I^- redox electrolyte and its corrosive nature deteriorates the long term stability of DSSCs.[3] To diminish the production cost the first attempt to replace a more fragile, less abundant, highly expensive, photo inert conducting glass with stainless steel (SS) substrate. SS has added advantages in terms of low material cost, non fragile and electrical transference capability.[4] In second it is a prerequisite to develop a cheap catalytic material with good chemical stability and high electrocatalytic activity.

By addressing this issue, Several carbonaceous materials (activated carbon, graphite, carbon nanotubes and carbon black)[5] metal sulphides,[6] conducting polymers[7] have been employed as catalysts for CE in DSSCs. Polyaniline (PANI) has been studied as a promising candidate for DSSCs due to its unique properties including high conductivity, good environmental stability, low cost, doping, and de-doping property and high catalytic activity for I_3^- reduction.[8]

Several researches are conducted to improve the processability and catalytic activity of PANI, and they include incorporation of different dopants,[9] varying the polymerization techniques,[10] surfactant addition[11] and composites with graphene.[12] Incorporation of constituent in the polymer skeleton is a common technique to synthesize polymers having improved properties.[13]

In the investigation of poly(ortho-methoxyaniline) (POA), a derivative of PANI which was investigated due to (a) the monomer *o*-anisidine is commercially available at low cost and has quite good solubility in water due to the methoxy group substituted at ortho-position of aniline (b) methoxy ($-OCH_3$) group diminishes the percentage of undesirable "ortho" coupling (c) higher polymerization yields with more regular structure of polymer.[14] Basanayaka *et al.*, studied graphene substituted POA nanocomposite for supercapacitor applications.[15] Savale *et al.* adopted the POA for glucose biosensor[16] Kulkarni *et al.* studied camphour sulphonic acid dopped POA in humidity sensor.[17] Kilmartin *et al.*[18] report the better corrosion inhibition of SS using POA. To the best of our knowledge, the structural and catalytic behavior of poly(*o*-anisidine) as CE material in DSSC is yet to be explored.

Here, we electropolymerize the POA through the employment of different nature of surfactants [non-ionic, polyoxyethylene (10) isooctylphenyl ether (TX), anionic sodium dodecyl

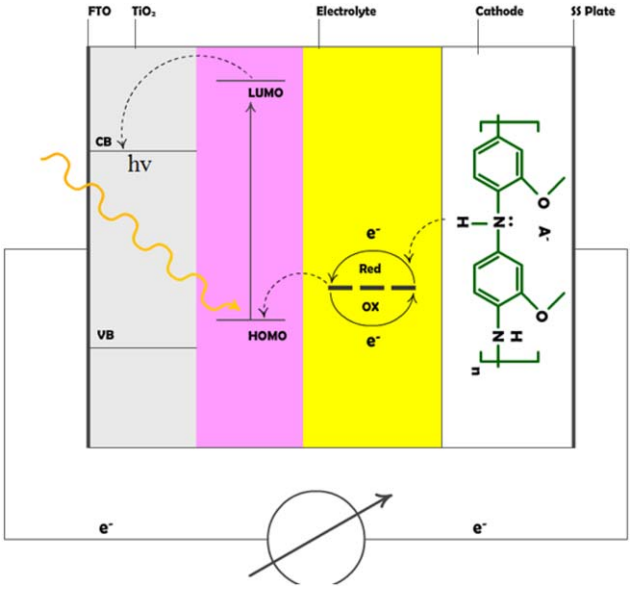

Figure 1. The operating principle of schematic representation of DSSCs. [Color figure can be viewed in the online issue, which is available at wileyonlinelibrary.com.]

sulphate (SDS) and cationic cetyl trimethyl ammonium bromide (CTAB)] as CE material for DSSCs. The Polymeric stabilizers (surfactant) have great influence on the structure, and to improve the properties with respect to stability, solubility in organic solvents, and processibility.[8] The morphology, doping degree, electrochemical impedance and the electrocatalytic activity of the CEs for the triiodide reduction reaction are discussed. Finally, DSSCs employed with these electrodes were fabricated and the cell efficiency was investigated.

EXPERIMENTAL

Materials

o-Anisidine (S-d fine) monomer was distilled under vacuum before use. SDS (LOBA Chemie), CTAB (S-d fine), TX (S-d fine) was used as received. The Degussa (P25), TiO_2 (Acros Organics), FTO glass, 4-*tert*-butylpyridine (TBP) (Aldrich), Lithium iodide (LiI) (Alfa Aesar), Lithium per chlorate ($LiClO_4$), I_2 (S-d fine) and Rose Bengal (Hi-media) were purchased from the scientific companies. Double distilled water was used were used for all experiments. Acetonitrile (Aldrich) was used without further purification.

POA films were grown by potentiodynamic polymerization by scanning the voltage linearly between −0.2 and 1.0 V versus Ag/AgCl at a scan rate at 100 mV s^{-1} for 25 cycles in aqueous solutions of POA. Before polymerization SS 304 plate was rinsed with deionized water and then immersed in ethanol, acetone and ultrasonically for 15 min. A one-compartment cell with a three-electrode system containing SS plate served as the working electrode, Ag/AgCl as the reference electrode, while Pt served as the CE. The electro polymerization solution composed of 0.1*M* *o*-anisidine, 0.1*M* H_2SO_4, for without surfactant POA (POA/NEAT) and addition of SDS, TX, and CTAB surfactants make POA/SDS, POA/TX, and POA/CTAB counter electrode. After deposition, the coated POA films were rinsed with 0.1*M* H_2SO_4 in order to remove soluble monomeric species.

Characterisation of the Electrode

The surface morphology was inspected by scanning electron microscopy (SEM) using SCi-QuantaFEG 250. Polymerization experiments and cyclic voltammogram measurements were performed on Autolab PGSTAT 30 (EcoChemi, the Netherlands). The electrochemical impedance spectroscopy (EIS) measurement were performed with the symmetrical cell consisted of two identical electrodes in an Autolab PGSTAT 30 (EcoChemi, The Netherlands) at the frequency range of 0.1–10^5 Hz. The magnitude of the alternative signal was 5 mV. The inter-electrode space was filled with electrolyte which was same as the one used in the assembly of DSSC. X-ray diffraction pattern of the sample was recorded using X'Pert–PRO X-ray diffractometer with Cu-Kα radiation. The photocurrent–voltage (*I–V*) characteristics of the assembled DSSCs were evaluated using the solar simulator (150 W Simulator, PEC-L11) under air mass 1.5 with 100 mW cm^{-2} light intensity.

Fabrication of DSSCs

FTO glass substrate were cleaned with deionized water and anhydrous ethanol and ultrasonic for 15 min. TiO_2 slurry was prepared by the vigorous grinding of 2 mL aqueous polyethelene glycol solution with 0.5 g of TiO_2 powder. The thin films of TiO_2 (P25 Degussa) were produced by doctor blade technique from a colloidal paste of TiO_2, followed by sintering step at 450°C for 30 min. The thickness of the TiO_2 film was about 10 μm. The TiO_2 film was preheated at 120°C for 30 min and then immersed into 0.3 m*M* Rose Bengal in ethanol for overnight. Afterwards, the electrode was washed with ethanol and then dried in air. The sandwich-type solar cells consisted of a dye-sensitized TiO_2 film as working electrode, POA as CE, and an electrolyte containing 0.5*M* LiI, 0.05*M* I_2, 0.5*M* *t*-butyl pyridine in acetonitrile solution. Lastly, the sandwich type DSSC was fabricated by clamping the CE on the top of the TiO_2 photoelectrode and electrolyte was inserted and sealed.

RESULTS AND DISCUSSION

Figure 1 illustrates the operating principle of DSSCs follows that the Rose Bengal (RB) (sensitizer) absorbs a photon of light to generate the photoexcited (RB*) [eq. (1)]. The photoexcited (RB*) injects an electron into the conduction band of TiO_2 [eq. (2)]. These electrons percolate through the TiO_2 film and are collected by the conducting substrate. The resultant oxidized sensitizer is then reduced back to its original state by electron injection from I^- ions in redox mediator [eq. (3)]. The I^- ion is regenerated by the reduction of triiodide ion I_3^- at the CE through the donation of electrons from the external circuit [eq. (4)] and then the circuit is completed.[19]

$$RB + h\nu \rightarrow RB* \text{ (absorption)} \quad (1)$$

$$RB* \rightarrow RB^+ + e^- \ (TiO_2) \text{ (electron injection)} \quad (2)$$

$$2RB^+ + 3I^- \rightarrow 2RB + I_3^- \text{ (regeneration)} \quad (3)$$

$$I_3^- + 2e^- \rightarrow 3I^- \quad (4)$$

To achieve higher efficiency, one of the eligible requirement is the redox reaction rate on CE should be fast [eq. (4)]. That

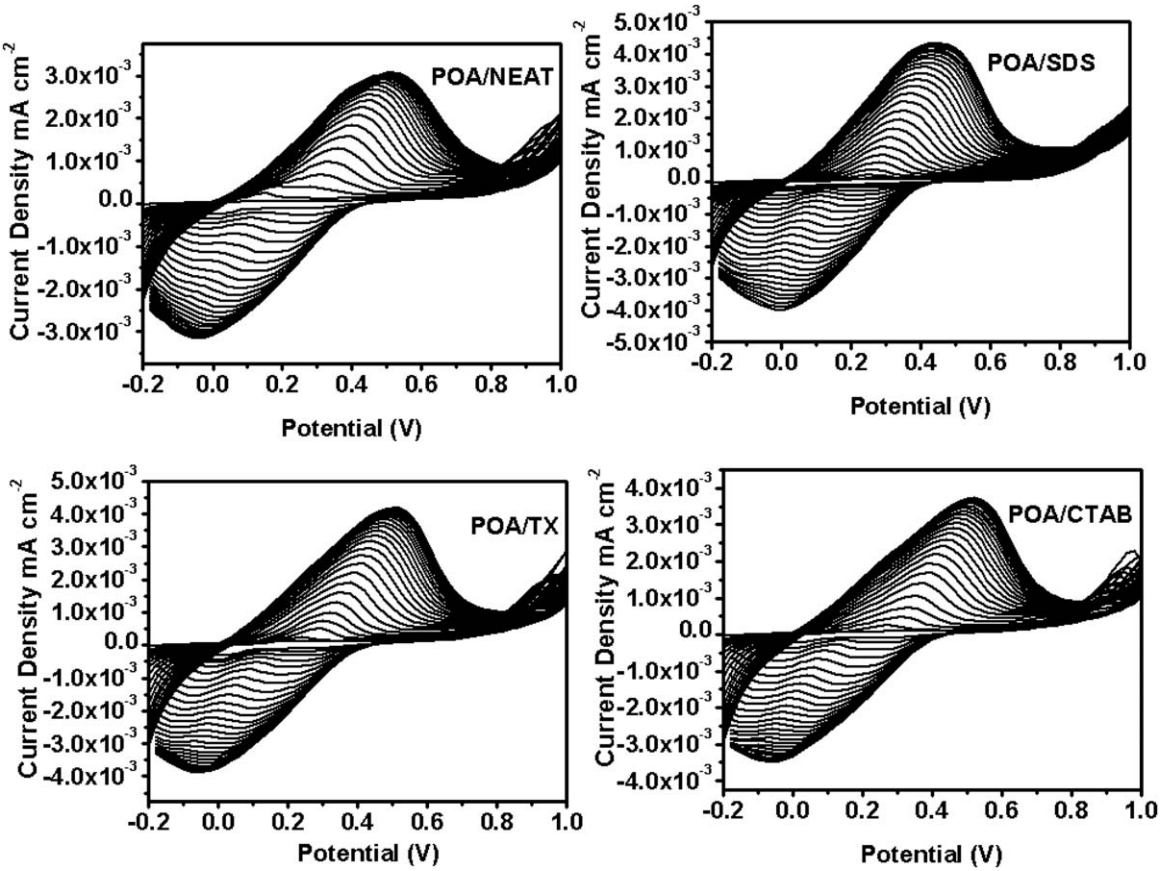

Figure 2. Electrodeposition of 25 cycles of various surfactant assisted POA by CV on SS plate.

means it should have higher catalytic activity in I_3^-/I^- redox reaction.[16]

Syntheses of Poly(o-anisidine) Film Counter Electrodes

The potentiodynamic deposition of different nature (anionic, neutral and cationic) of surfactant assisted POA film was scanned for 25 cycles as shown in Figure 2. The oxidation of POA arises at about +0.25 V is corresponds to the conversion of amine units into radical cation. The entire polymer deposit at the electrode surface is relative only to anodic current density at 0.25 V.[20,21] The redox peak currents gradually increase with the number of cycles, indicating growth of conducting polymer film in each case.

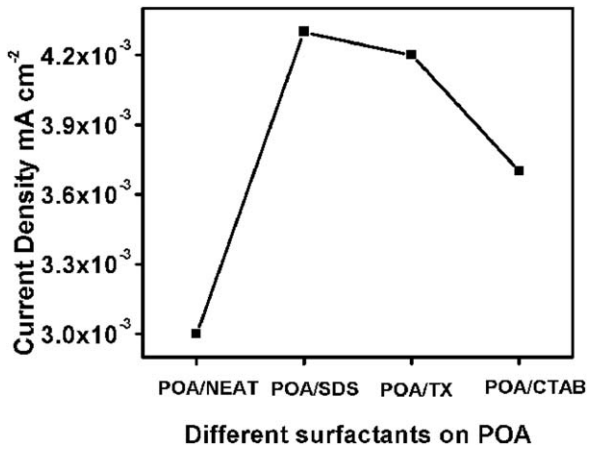

Figure 3. Current enhancement during cyclic voltammetric growth of POA and different nature of surfactant assisted POA.

Current density during cyclic voltammetric growth of POA at different nature of surfactant assisted POA are shown in Figure 3. The highest current densities corresponding to the anodic peaks are observed for the POA-SDS. The rate of film growth as expressed by the peak current is several-fold higher in SDS surfactant assisted POA compared to POA-TX, POA-CTAB, and POA-NEAT. The enhanced growth of POA-SDS is due to anionic part of SDS can act as a growth controller, as well as an agglomeration inhibitor and dopant.

Surface Morphology of Poly(*o*-anisidine) Film

SEM images of POA counter electrodes are shown in Figure 4. The SEM image of Figure 4a shows POA/NEAT which have small cage like morphology on the surface of the SS plate. For POA/CTAB there was repulsion between positive charge anisidine and cationic part of CTAB and is in agreement with the CTAB surfactant deposit on the surface as white particle in Figure 4(b). POA/TX shows an irregular sponge like morphology in Figure 4c. For both cationic and neutral surfactant the necessary local environment for the electrochemical micelle synthesis of conducting polymer does not exist.[22] The surfactant assisted polymer synthesis resulted in controlled morphology of different

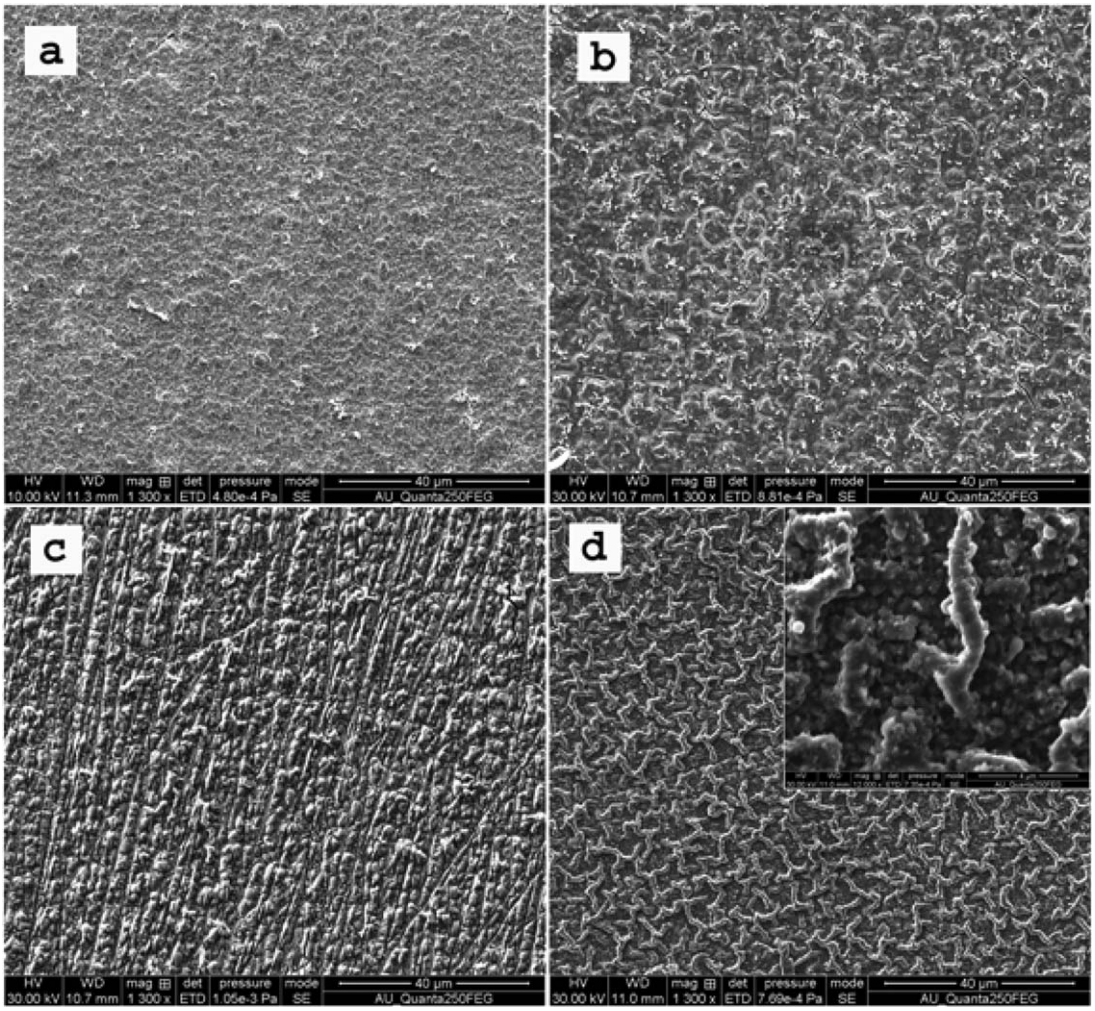

Figure 4. SEM images of (a) POA/NEAT, (b) POA/CTAB, (c) POA/TX, (d) POA/SDS.

micro/ nanostructures depending on the nature of the surfactant.[23,24]

POA-SDS in Figure 4(d) demonstrates nanofibrillar morphology with a number of nanoparticles attached on the surface of the POA nanorods inset figure in Figure 4(d) leads to high surface area. The high active site of POA-SDS nanofilm can facilitate the diffusion of redox couple in the CE. Since SDS molecules can act both as dopant and surfactant during electropolymerization. Polymeric nanostructures are formed on surfaces due to combination of interfacial, intra- and intermolecular forces.[25]

Impedance Analysis

Impedance analysis (EIS) measurement was performed in a dummy cell contain two identical CEs and using the electrolyte same for the DSSCs. Nyquist plots of different surfactant assisted POA CE and their equivalent circuit are shown in Figure 5 which demonstrates a semicircle at high frequency region, corresponds to the charge-transfer resistance (R_{ct}) and the corresponding chemical capacitance (CPE) of the electrode/electrolyte interface. Spike at low frequency region refers to the Nernst diffusion impedance (W). The above two region correspond to two different electrochemical reactions are possible in this arrangement. The R_{ct} of the dummy cell was estimated by taking half of the diameter of its corresponding semicircle.

From Table I, a slight decrease of R_s value, from POA/NEAT-CE to POA/SDS, which is responsible for the enhanced charge-transfer ability of CEs. The shrink in R_{ct} responsible for the diffusion of the redox couples within the higher surface area and well aligned structure accelerated by the active sites. Moreover R_{ct} varies inversely with the electrocatalytic activity for the reduction of I^-/I_3^- redox species.[26] The R_{ct} value of POA/SDS CE is (49 Ω cm^2) two times smaller than that of pure POA/NEAT and lower value to that of POA/TX (68 Ω $cm^{2)}$ and POA/CTAB (71 Ω cm^2). The enormous decrease of POA/SDS was due to higher surface area, electro catalytic activity and well aligned nanofibre structure. As expected the bare SS plate shows no charge-transfer resistance indicating that it show no electrocatalytic activity.

X-ray Diffraction Analysis

The X-ray diffraction pattern of the synthesized CEs was represented in Figure 6. In the XRD pattern reflections at 45°, 52°, and 75° corresponding to the SS plate.[27] For POA a broad peak occurred at $2\theta\sim$ 25.6 is amorphous in nature can be ascribed to

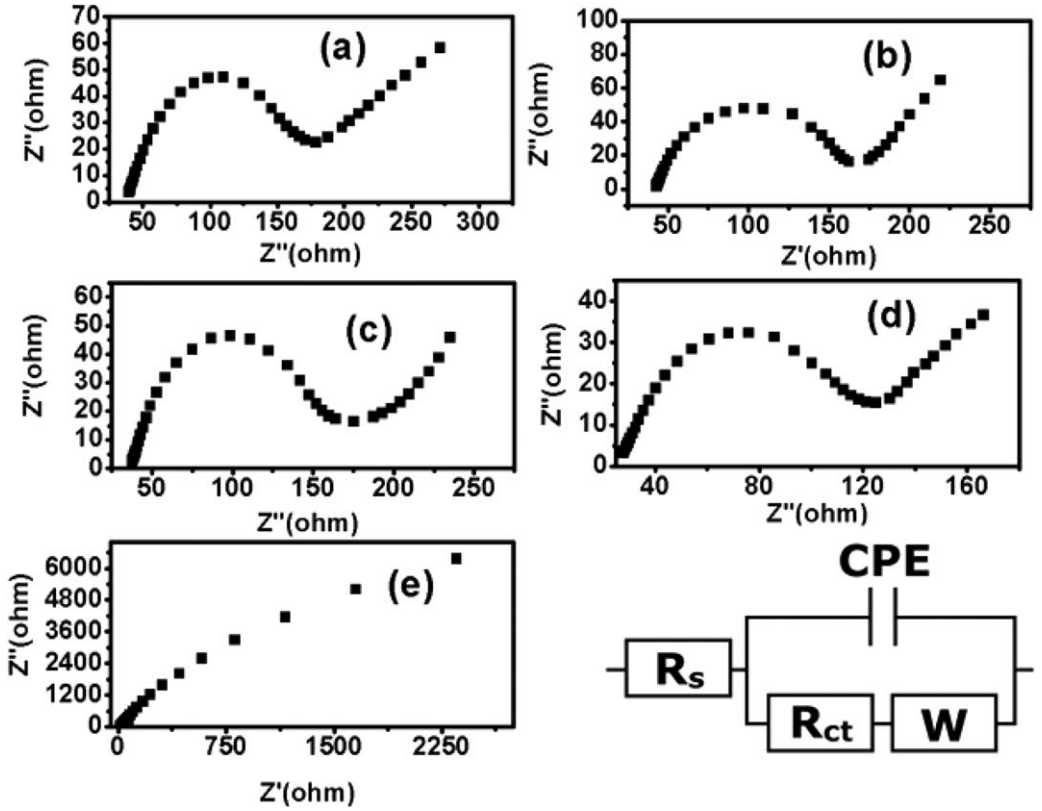

Figure 5. Impedance spectra of (a) POA/NEAT, (b) POA/TX, (c) POA/CTAB, (d) POA/SDS, (e) SS plate (f) equivalent circuit.

the periodicity parallel and perpendicular to the polymer chains of POA.[28] For POA/SDS, POA/TX and POA/CTAB a very small peak occurred at $2\theta \sim 25$ declares the crystalline nature of the polymer. And this is due to interaction of SDS, TX-100 and CTAB surfactants on structural properties of POA.

The Electrical Properties of CEs

Cyclic voltammetry (CV) was used to investigate the electrocatalytic activities of CEs. The CE in DSSC serves as an electrocatalyst for reducing I_3^- to I^-. It is well known that two reactions are possible for the CV of CE is anodic [eq. (5)] and cathodic reaction [eq. (6)] is

$$3I^- - 2e^- \rightarrow I_3^- \quad (5)$$

$$I_3^- + 2e^- \rightarrow 3I^- \quad (6)$$

The cathodic reduction peak current density in CV curves can be used to evaluate the electrocatalytic activity of the CEs. To achieve higher efficiency in DSSC, one of the eligible requirements is the higher reduction peak current density. If the reduction peak current density is higher the reduction rate on CE should be fast. From Figure 7(a,b), the cathodic reduction peak current densities for the samples are in the order: POA/SDS > POA/TX > POA/CTAB > POA/NEAT ~ POA/Pt. The redox current density of the POA-SDS CE was significantly higher than that of Pt and other POA CEs, indicating a much faster rate for I^-/I_3^- reaction can be demonstrated. The POA-SDS CE with more electrochemically active may largely be due

Table I. Best-Fit Values for *Rs*, R_{ct}, of the Equivalent Circuit in Figure 5f

CEs	R_s (Ω cm^2)	R_{ct} (Ω cm^2)	W (Ω cm^2)
POA/NEAT	38	82	120
POA/CTAB	43	71	78
POA/TX	37	68	87
POA/SDS	27	49	45

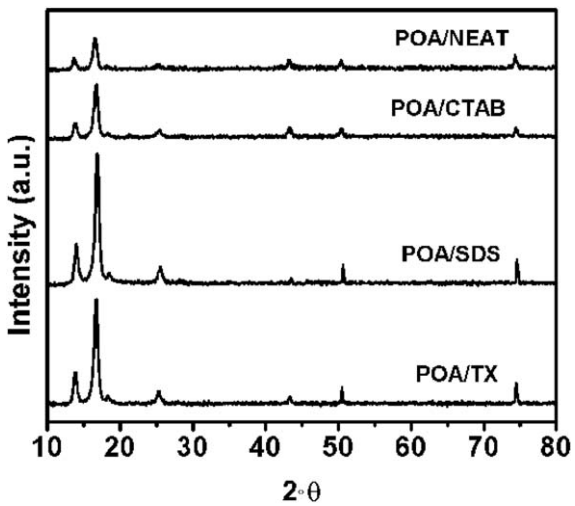

Figure 6. The XRD pattern of POA CEs.

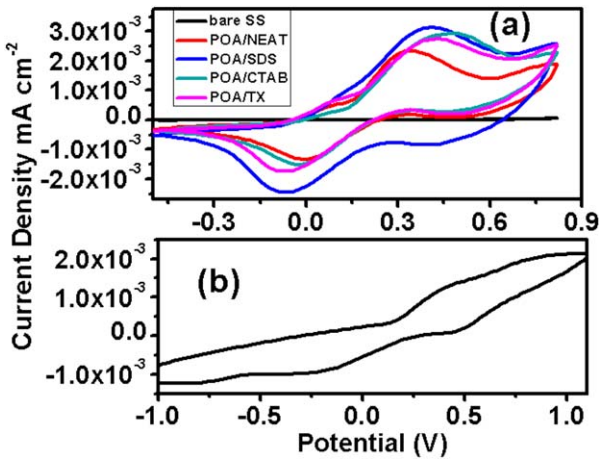

Figure 7. Cyclic voltammogram of POA (a) and Pt (b) CEs. [Color figure can be viewed in the online issue, which is available at wileyonlinelibrary.com.]

to its high active surface, which is in agreement with the SEM and EIS results.

Figure 8(a) illustrates the relationship between the redox peak current density of POA-SDS and the square root of scan rates

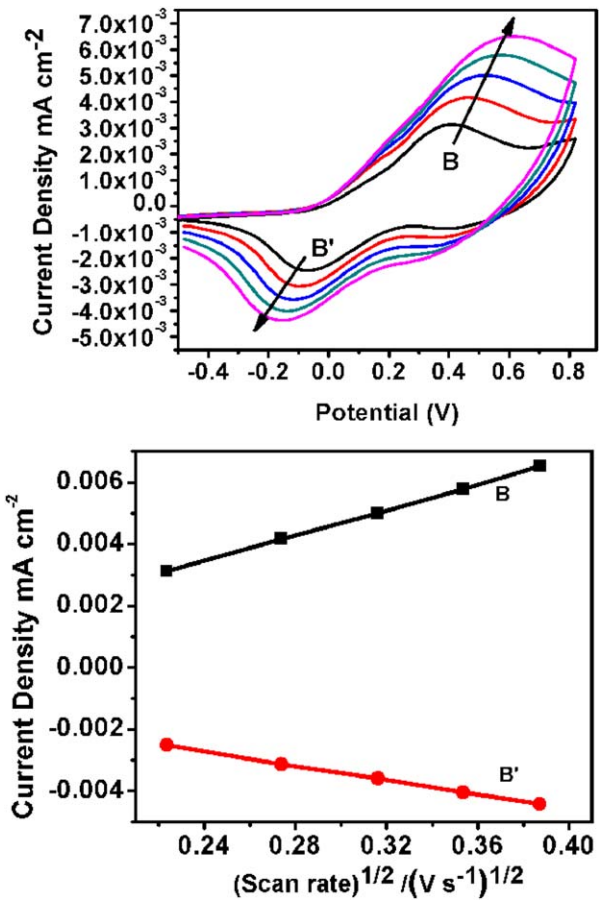

Figure 8. (a) Cyclic voltammogram for the POA/SDS CE with scan rate from (from inner to outer; 50, 75, 100,125,150 respectively), (b) Relationship between redox peak current and scan rate. [Color figure can be viewed in the online issue, which is available at wileyonlinelibrary.com.]

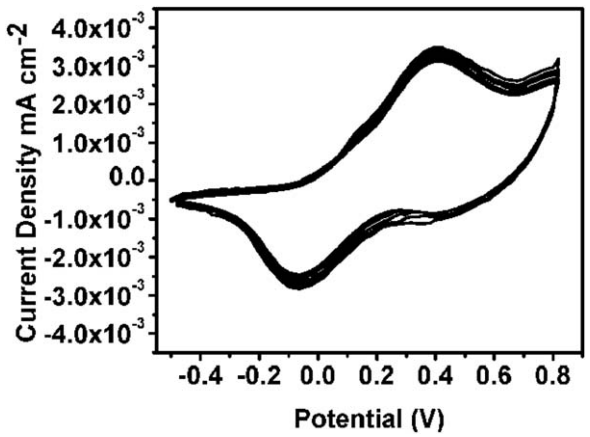

Figure 9. Consecutive ten cyclic voltammogram of POA/SDS CE.

in acetonitrile solution. Both the cathodic and anodic peak current density increase approximately linearly proportional to the square root of the scan rate. A good linear relationship of POA-SDS indicates that the redox reaction of I^-/I_3^- on electrodes is controlled by ionic diffusion of the electrolyte and indicating an adsorption-controlled electrode process, which is related to the transport of iodide species inside the POA/SDS film as well as in the bulk solution.[29] The linearity of the peak current densities with the square root of scan rates in Figure 8(b) indicates that charge transfer in the redox step is empirically controlled by the diffusion of charges in the films as described by Randles-Sevcik theory:[30]

$$i_p = (2.69\times10^5)\, n^{3/2} C^b A D^{1/2} v^{1/2}$$

where n is the number of electrons, A is the surface area of the electrode (cm^2), D is the diffusion constant (cm^2/s), C^b is the bulk concentration of electroactive species (mol/cm^3), and v is the scan rate (V/s). Therefore, for a diffusion-controlled process, the peak current is proportional to the square root of the scan rate. In the consecutive 10 cycles test, the CVs did not change, and exhibited stable anodic (i_{pa}) and cathodic (i_{pc}) peak current densities as shown in Figure 9 indicating that the POA-SDS

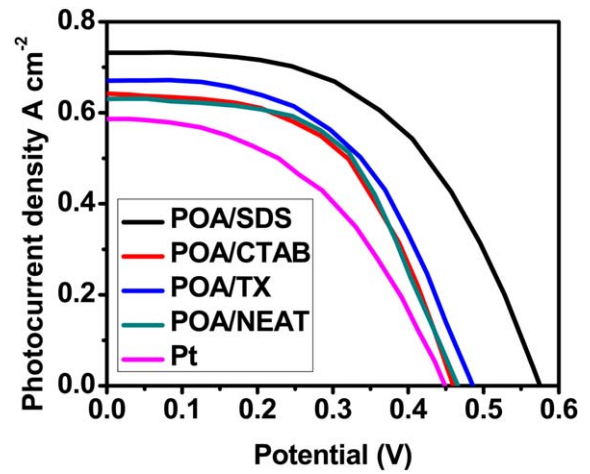

Figure 10. J–V curves of the DSSCs based on POA and Pt CEs. [Color figure can be viewed in the online issue, which is available at wileyonlinelibrary.com.]

Table II. Photovoltaic Parameters of DSSCs Based on Pt and POA CEs

Counter electrode	J_{sc} (A/cm^2)	V_{oc} (V)	FF	η%
Pt	0.6991	0.5602	0.53	2.0
POA/NEAT	0.6331	0.4982	0.53	1.67
POA/TX	0.6629	0.4998	0.55	1.82
POA/CTAB	0.6424	0.4812	0.55	1.70
POA/SDS	0.7322	0.6018	0.57	2.50

film was not only with excellent electrochemical stability in addition to that it was also attached tightly and uniformly on the SS substrate.

Photovoltaic Performances

The photovoltaic characteristics of DSSCs with different nature of surfactant assisted POA and Pt counter electrode are shown in Figure 10, and the detailed photovoltaic parameters of the devices are summarized in Table II. POA/SDS nanofiber CE achieves higher J_{sc} than that of other fabricated CE. This might be attributed, which provides larger active surface area can accelerate the tri-iodide recovery. The optimal POA/SDS significantly improves the charge-transfer ability, which possibly will be a main factor in enhancing the photocurrent density of a DSSC cell. Due to poor catalytic activity, the DSSC with POA/NEAT and other surfactant assisted electrodes exhibited lowest FF, J_{SC}, and $\acute{\eta}$. It can be concluded that the photovoltaic performance is an agreement with CV and EIS results.

CONCLUSION

Surfactant assisted POA counter electrode (CE) was successfully prepared on SS substrate by potentiodynamic method. SDS introduced into the POA preparation causes controllable synthesis of nanofiber like morphology. Here SDS can act as surfactant as well as doping agent. The electrochemical growth peak current, charge-transfer resistance and catalytic property of these films is several-fold improved compared to the values obtained on pure POA and other surfactant doped POA. DSSCs based on POA/SDS CE achieved an overall light-to electric energy conversion efficiency of 2.5%.

ACKNOWLEDGMENTS

Dr. TS thankful to University Grants Commission, New Delhi, India, for financial support under major research project fund (F. No: 40-72/2011(SR) dated: 05.7.2011).

REFERENCES

1. Calogero, G.; Calandra, P.; Irrera, A.; Sinopoli, A.; Citro, I. D.; Marco, G. *Energy Environ. Sci.* **2011**, *4*, 1838.
2. Yun, S.; Wang, L.; Guo, W.; Ma, T. L. *Electrochem. Commun.* **2012**, *24*, 69.
3. Murakami, T. N.; Grätzel, M. *Inorg. Chim. Acta* **2008**, *361*, 572.
4. Chena, C.-M.; Chena, C.-H.; Wei, T.-C. *Electrochim. Acta* **2010**, *55*, 1687.
5. Lee, K.-M.; Chiu, W.-H.; Wei, H.-Y.; Hu, C.-W.; Suryanarayanan, V.; Hsieh, W.-F.; Ho, K.-C. *Thin Solid Films* **2010**, *518*, 1716.
6. Lin, J.-Yu.; Liao, J.-H.; Chou, S.-W. *Electrochim. Acta* **2011**, *56*, 8818.
7. Lin, Z. P.; Ye, B. X.; Hu, X. D.; Ma, X. Y.; Zhang, X. P.; Deng, Y. Q. *Electrochem. Commun.* **2009**, *11*, 1768.
8. Qiu, Y.; Lu, S.; Wang, S.; Zhang, X.; He, S.; He, T. *J. Power Source.* **2014**, *253*, 300.
9. Li, Z.; Ye, B.; Hu, X.; Ma, X.; Zhang, X.; Deng, Y. *Electrochem. Commun.* **2009**, *9*, 1768.
10. Zhang, J.; Hreid, T.; Li, X.; Guo, W.; Wang, L.; Shi, X.; Su, H.; Yuan, Z. *Electrochim. Acta* **2010**, *55*, 3664.
11. Park, S. H.; Shin, K.-H.; Kim, J.-Y.; Yoo, S. J.; Lee, K. J.; Shin, J.; Choi, J. W.; Jang, J.; Sung, Y. E. *J. Photochem. Photobiol. A Chem.* **2012**, *245*, 1.
12. Niu, H.; Qin, S.; Mao, X.; Zhang, S.; Wang, R.; Wan, L.; Xu, J.; Miao, S.; sleeve, A. *Electrochim. Acta* **2014**, *121*, 285.
13. Gok, A.; Stova, M.; Yavuz, A. G. *Synth. Met.* **2007**, *157*, 23.
14. Valle, M. A.; Gacitúa, M. A.; Borrego, E. D.; Zamora, P. P.; Díaz, F. R.; Camarada, M. B.; Antilén, M. P.; Soto, J. P. *Int. J. Electrochem. Sci.* **2012**, *7*, 2552.
15. Basanayaka, P. A.; Ram, M. K.; Stefanakos, L.; Kumar, A. *Mater. Chem. Phys.* **2013**, *141*, 263.
16. Savale, P. A.; Shirsat, M. D. *Appl. Biochem. Biotech.* **2009**, *159*, 299.
17. Kulkarni, M. V.; Viswanath, A. K. *Sens. Actuators, B: Chem.* **2005**, *107*, 791.
18. Kilmartin, P. A.; Trier, L.; Wright, G. A. *Synth. Met.* **2002**, *131*, 99.
19. Mishra, A.; Fischer, R.; Uerle, P. B. *Angew. Chem. Int. Ed.* **2009**, *48*, 2474.
20. Patil, S.; Mahajan, J. R.; More, M. A.; Patil, P. P.; Gosavi, S. W.; Ganga, S. A. *Polym. Int.* **1998**, *46*, 99.
21. Ozyilmaz, A. T.; Ozyilmaz, G. *Prog. Org. Coat.* **2010**, *67*, 28.
22. Liu, W; Kumar, J.; Tripathy, S. *Langmuir* **2002**, *18*, 9696.
23. Chandrasekaran, S.; Srinivasan, P; Frederic, C. *Mater. Lett.* **2008**, *62*, 882.
24. He, B.; Tang, Q.; Wang, M.; Ma, C.; Yuan, S. *J. Power Source* **2014**, *256*, 8.
25. Khan, R. *Adv. Chem. Eng. Sci.* **2011**, *1*, 140.
26. Wu, J.; Li, Y.; Tang, Q.; Yue, G.; Lin, J.; Huang, M.; Meng, L. *Sci. Rep.* **2014**, *4028*, 1.
27. Leoni, M.; Scardi, P.; Rossi, S.; Fedrizzi, L.; Massiani, Y. *Thin Solid Films* **1999**, *345*, 263.
28. Zhang, L.; Peng, H.; Sui, J.; Soeller, C.; Kilmartin, P. A.; Sejdic, J. T. *J. Phys. Chem. C* **2009**, *113*, 9128.
29. Wang, S.; Lu, S.; Li, X.; Zhang, X.; He, S.; He, T. *J. Power Sources* **2013**, *242*, 438.
30. Xiao, Y. M.; Lin, J. Y.; Tai, S. Y.; Chou, S. W.; Yue, G. T.; Wu, J. H. *J. Mater. Chem.* **2012**, *22*, 19919.